RAA 2015 Vol. **15** No. **12**, 2173–2186 doi: 10.1088/1674–4527/15/12/005
http://www.raa-journal.org *http://www.iop.org/journals/raa*

Research in Astronomy and Astrophysics

Time delay and extended halo for constraints on the intergalactic magnetic field

Yuan-Pei Yang and Zi-Gao Dai

School of Astronomy and Space Science, Nanjing University, Nanjing 210093, China; *dzg@nju.edu.cn*
Key Laboratory of Modern Astronomy and Astrophysics (Nanjing University), Ministry of Education, Nanjing 210093, China

Received 2015 April 8; accepted 2015 May 29

Abstract Primary gamma rays emitted from extragalactic very-high-energy (VHE) sources, such as blazars, will generate cascade radiation in intergalactic space with a scale of $\sim 100\,\mathrm{Mpc}$, for $z \sim 0.1$ and $E_\gamma \sim 1\,\mathrm{TeV}$. These cascades proceed through electron-positron pair production and inverse Compton (IC) scattering in the cosmic background radiation fields, mainly cosmic microwave background (CMB) radiation and extragalactic background light in the voids of the universe. The existence of an intergalactic magnetic field (IGMF) would deflect paths of electron-positron pairs that scatter CMB photons, causing some observable effects, such as time delay, an extended halo, and a spectral change. Here we reanalyze the diffusion of an electron jet deflected by IGMF and propose a unified semi-analytical model. By using publicly available data from the Fermi/LAT detector and contemporaneous TeV observations, we find that the cascade photon flux is not significantly affected by the IGMF strength for non-variable blazars when the IGMF is weaker than $\sim 10^{-16}\,\mathrm{G}$. This result is clearly different from previous works that analyzed the extended halo and time delay separately for non-variable blazars and flaring blazars. By applying our model to two extreme blazars (1ES 0229+200 and 1ES 1218+304), we obtain the IGMF lower limit of order $\gtrsim 10^{-13} \sim 10^{-14}\,\mathrm{G}$ in the non-variable case, which is a stronger constraint on the IGMF strength than previous works ($\gtrsim 10^{-16} \sim 10^{-18}\,\mathrm{G}$), and $\gtrsim 10^{-18} \sim 10^{-19}\,\mathrm{G}$ in the case of flaring blazars. Furthermore, we study the light curves and extended halo of the cascade photons by considering the effects of the IGMF.

Key words: gamma rays: general — galaxies: magnetic field — galaxies: individual (1ES 0229+200, 1ES 1218+304)

1 INTRODUCTION

The measurement of the intergalactic magnetic field (IGMF) is helpful for understanding the large scale structure of the universe and the origin of the galactic magnetic field. The magnetic fields of galaxies and galaxy clusters in the range of $\sim 10\,\mu\mathrm{G}$ are measured via recent observations of Faraday rotation (Kronberg 1994; Han et al. 2006; Bonafede et al. 2009; Jansson & Farrar 2012). Theoretically, the observed galactic magnetic field is generally believed to result from the $\alpha - \omega$

amplification mechanism of weaker seed fields (Widrow 2002; Kulsrud & Zweibel 2008), similar to the explanation of the origin of other strong magnetic objects (e.g., magnetars). Kulsrud & Zweibel (2008) proposed that the seed fields could be generated via the Biermann battery mechanism (Biermann 1950), Harrison mechanism (Harrison 1970), or some others. The Biermann battery mechanism emphasizes that the seed fields are generated in protogalaxies following the condition of a finite angle between density gradients and pressure gradients, resulting from first supernovae, activity of active galactic nuclei (AGN), gravitational collapse, turbulence, and so on. However, it is hard to know whether such processes in protogalaxies could efficiently make magnetic fields fill the voids (Zweibel 2006). On the other hand, the Harrison mechanism invokes rotating structures in the early universe, in which the differential rotation of relativistic electrons and non-relativistic protons produces the earlier magnetic fields of the universe (Widrow 2002). Because of the development of γ-ray astronomy, the detection of the IGMF has provided valuable insights for understanding significant problems in the origin of the IGMF and associated physical processes in the early universe.

The existing measurements of cosmic microwave background (CMB) anisotropies, Faraday rotation of the radio emission of quasars, Zeeman splitting, and ultrahigh energy cosmic rays indicate that the upper limit of the IGMF is $B_{\rm IGMF}\lambda_{\rm coh}^{1/2} \ll 10^{-9} \sim 10^{-10}\,{\rm Mpc}^{1/2}{\rm G}$, for $\lambda_{\rm coh} \lesssim 1\,{\rm Mpc}$ (Neronov & Semikoz 2009). In the past decades, no method gave direct measurements or lower limits of IGMF. Until recently, more and more extragalactic very high energy (VHE) sources could be used to detect the IGMF. In principle, the IGMF could be measured by cascade radiation from extragalactic TeV sources, including blazars and a few radio galaxies and starburst galaxies (Plaga 1995; Dai et al. 2002; Fan et al. 2004; Razzaque et al. 2004; Murase et al. 2008; Ichiki et al. 2008; Takahashi et al. 2008, 2011; Neronov & Semikoz 2009; Takahashi et al. 2012). TeV photons from an extragalactic source interact with infrared (IR)/ultraviolet (UV) photons of the extragalactic background light (EBL), which generate e^+e^- pairs, losing their energy through inverse Compton (IC) scattering in the CMB. In this process, if the primary spectrum extends up to a VHE band, a fraction of the reprocessed emission will still be above the pair-production threshold, leading to the second generation of pairs. However, if the cascade process develops in the void of the universe, the IGMF that deflects the paths of cascading electron-positron pairs would modify the properties of the secondary radiation, causing some observable effects, such as time delay (Plaga 1995; Dai et al. 2002; Takahashi et al. 2008; Murase et al. 2008; Takahashi et al. 2012, 2013) and extended gamma-ray halos (Dolag et al. 2011; Tavecchio et al. 2010; Neronov & Vovk 2010; Tavecchio et al. 2011), which can be used to infer the bounds of the IGMF strength.

In order to detect the IGMF via the cascade radiation of VHE sources, we should know the properties of the primary radiation of the VHE sources. TeV blazars, as extragalactic VHE sources, are often treated as a probe of the IGMF and the EBL. Blazars are the most extreme kind of AGN, which are characterized by a relativistic jet closely aligned with the observer's line of sight. The spectral energy distribution (SED) with two broad peaks is the most outstanding feature of blazars, which extends from radio to γ-ray energies. The first peak in the IR/UV or even X-ray band is attributed to synchrotron emission by ultra-relativistic electrons in the jet, and the second peak, mainly covering X-ray or γ-ray energies, is generally proposed to be produced through IC scattering by the same electrons responsible for the synchrotron emission, which is the synchrotron-self-Compton (SSC) mechanism. However, for some hard TeV blazars, such as 1ES 0229+200 or 1ES 1101-232, the external-Compton (EC) mechanism (Böttcher et al. 2008) or proton-induced cascade emission (Essey et al. 2010; Essey & Kusenko 2010; Essey et al. 2011; Murase et al. 2012) are proposed to explain these hard TeV observations well. Fossati et al. (1998) first indicated that there is an inverse relation between the frequencies of both peaks and the luminosity for blazars. The high-energy bump of high-frequency peak blazars (also called high-frequency BL Lacs or HBLs), with $\nu_{\rm syn} \gtrsim 10^{17}{\rm Hz}$, can reach the TeV band, although their γ-ray luminosity is much smaller than the synchrotron luminosity. However, there are two special cases for TeV blazars: first, some HBLs show a γ-ray dominated SED during their strong flares, and second, some special TeV blazars appear to have non-

variable and high TeV flux during observations that span several years. Both kinds of TeV blazars with high γ-ray luminosity are useful for constraining the EBL and IGMF.

The properties of the cascade emission spectrum are the key to constraining the IGMF. Dai et al. (2002), Murase et al. (2008) and Takahashi et al. (2012) focused on the discussion of variable GeV emission, a byproduct of the cascade emission of the primary TeV emission of a rapidly flaring blazar. A similar method has been applied to the emission from γ-ray bursts (Dai & Lu 2002; Razzaque et al. 2004; Takahashi et al. 2008). For non-variable TeV blazars, such as 1ES 0229+200, Neronov & Vovk (2010), Tavecchio et al. (2010) and Tavecchio et al. (2011) considered that the low energy GeV cascade photons, along the direction of deflecting electron-positron pairs, would not be included in the point spread function (PSF) of Fermi/LAT, and derived the lower limit on the IGMF strength to be on the order of $10^{-16}\,\mathrm{G}$. In fact, the observed flux at the GeV band consists of the primary flux and the cascade flux. If the intrinsic spectrum is not so hard, the cascade flux would be lower than the primary flux, even ignoring the IGMF. Vovk et al. (2012) analyzed the spectral index of the primary emission and the EBL uncertainty for constraining the IGMF.

In previous works, it was assumed that the observed TeV photons' opening angle θ_j of blazars is much smaller than the electron deflection angle θ_B. Here, $\theta_j = \max(\theta_{j,0}, 1/\Gamma_B)$, where $\theta_{j,0}$ is the initial bulks' jet angle and Γ_B is the Lorentz factor of the bulk of the blazar. In this case, the cascade flux would be effectively diffused due to the deflection of electron-positron pairs in IGMF. However, for $\theta_j \gg \theta_B$, the diffusion of the observed cascade flux would not be effective. This is because all of the observed cascade photons are produced by the electron-positron pairs that are emitted from the angle θ_B. The electron-positron pairs outside θ_B would be deflected within the observed angle. In this case, the suppression of IGMF would be weaker, leading to a stronger lower limit of IGMF.

In this paper, we reanalyze the diffusion of an electron jet deflected by IGMF and find that the cascade photon flux is not significantly affected by the strength of IGMF for non-variable blazars when the strength of IGMF is so weak that the jet opening-angle is larger than the deflection angle, as shown in Figure 1 and discussed in the next section. Thus we obtain a stronger constraint on the strength of IGMF than previous works, e.g. a lower limit of order $10^{-13} \sim 10^{-14}\,\mathrm{G}$ for 1ES 0229+200. This result is different from the previous works that analyzed the extended halo and time delay separately for non-variable blazars (Tavecchio et al. 2010, 2011) and flaring blazars (Takahashi et al. 2012, 2013). Here, we provide a unified interpretation for the time delay and extended halo in a semi-analytical model. We constrain the IGMF strength from both the measurement of the SED and the light curve of TeV blazars. For non-variable hard TeV blazars, such as 1ES 0229+200, there are no models that unequivocally explain the recent observations. We constrain the IGMF in a long range of lifetimes of TeV blazars, by assuming that their TeV luminosities are slowly varying during their lifetimes. We also analyze the VHE flare of 1ES 1218+304 on 2009 January 30. This TeV blazar has a hard index by considering the EBL absorption. However, the observation of Fermi/LAT did not show a remarkable flare in the GeV band, which could be explained by the suppression of the IGMF. For 1ES 0229+200, we use the data of three-year observations of H.E.S.S. (Aharonian et al. 2007) in the VHE band and the Fermi/LAT observation from January 2009 to May 2013. According to the VHE observations, 1ES 0229+200 shows a significant feature associated with non-variable hard TeV blazars, considering the absorption of the EBL. Dermer et al. (2011) obtained the IGMF lower limit to be of order $10^{-18}\,\mathrm{G}$, based on an assumption that TeV emission should be persistent for at least the past million years. In fact, most VHE sources are highly variable, with their TeV flux fluctuates by several orders of magnitude over timescales of a few years and less. Murase et al. (2012) proposed that fast variability should be produced in/near the blazar region, while for no rapid variability, the observed component may come from an extended jet, such as in the EC model. For 1ES 1218+304, we analyze the VHE flare on January 2009 (Acciari et al. 2010) and use contemporaneous Fermi/LAT data. Usually, VHE flares are quite common in many nearby blazars, such as Mrk 501 and Mrk 421, but the case of 1ES 1218+304 (redshift $z = 0.182$) is particularly interesting since it is a blazar that exhibits unusually hard VHE spectra considering its redshift. The

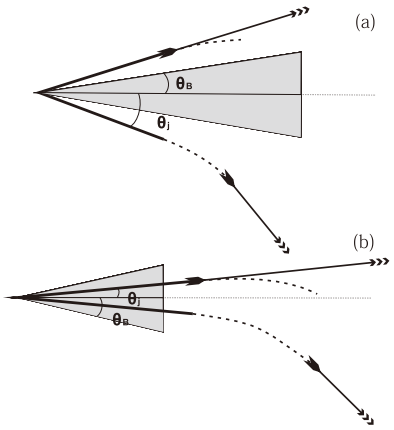

Fig. 1 A schematic diagram for an electron jet deflected by IGMF. The thick lines represent the intrinsic TeV photons, the dashed lines represent the cascade electrons (not including positrons, because their deflections are symmetrical in IGMF), and the arrows represent the GeV cascade photons. The gray area represents the deflection angle θ_B, in which only the TeV photons could produce the observed cascade photons. The gray area represents the deflection angle θ_B, (a) $\theta_j > \theta_B$, the photon flux emitted by electron-positron pairs with the same energies does not diffuse by the IGMF, because all observed cascade photons come from the gray area, and the other electrons outside θ_B would be deflected into it for the duration of the jet; (b) $\theta_j < \theta_B$, the cascade flux would be diffused by a factor, θ_j/θ_B, due to the fact that the jet angle of the blazar is diffused by IGMF to a larger angle θ_B.

day-scale flare of 1ES 1218+304 may imply shock acceleration scenarios in relativistic jets and in particular for the viability of kiloparsec-scale jet emission scenarios (Acciari et al. 2010).

This paper is organized as follows. In Section 2, we describe the physical process of cascade emission. In Section 3, we describe the data utilized in this paper. In Section 4, we present our numerical results. Section 5 presents some discussions and conclusions.

2 BLAZARS'S LIFETIMES AND THE IGMF

Primary high-energy γ-rays are emitted by charged particles via the SSC or EC mechanism, and a fraction of them can be absorbed in EBL as they travel toward the observer. Interactions of these TeV photons with EBL photons lead to the deposition of e^+e^- pairs in the voids, on a scale of $\gtrsim 100\,\mathrm{Mpc}$. These e^+e^- pairs emit secondary γ-rays via IC scattering off CMB photons. If an IGMF, which deflects electron and positron paths, is negligible when its strength is less than $10^{-25}\mathrm{G}$, then the IC photons from the cascade radiation would contribute to the primary GeV γ-ray flux. Otherwise, if the magnetic field along the path of the cascade development is strong enough to deflect the paths of the pairs, the cascade emission appears as an extended emission around the initial point source, leading to some low energy cascade photons that could not enter the detector's PSF. On the other hand, these deflecting paths lead to a long time decay for cascade photons, which would change the shape of the observed SED.

At first we summarize the basic physical process of the cascade emission. If primary photons of energy E_γ are absorbed by EBL, $E'_\gamma\,\epsilon' \gtrsim 2(m_\mathrm{e}c^2)^2$, the resulting e^+e^- pairs have Lorentz factors $\gamma_\mathrm{e} = E'_\gamma/2m_\mathrm{e}c^2 \approx 10^6(1+z)(E_\gamma/\mathrm{TeV})$ where m_e is the electron mass. Due to the absorption of EBL, this attenuation is above the critical γ-ray energy $E'_\mathrm{crit} \approx 170(1+z)^{-2.38}\,\mathrm{GeV}$ (Ackermann et al. 2012). Then the pairs will subsequently Compton scatter on the ambient CMB photons. As

a result, the initial energy of a CMB photon, $\bar{\epsilon}'$, is upscattered to an average value via IC. In the observer frame, $\sim \gamma_{\rm e}^2\bar{\epsilon}' \simeq 0.63(E_\gamma/1{\rm TeV})^2\,{\rm GeV}$, where $\bar{\epsilon}' = 2.7(1+z)kT$ is the mean energy of the CMB photons with $T \approx 2.7\,{\rm K}$.

Define the flux variation of blazars as $t_{\rm var}$. For fast variable blazars, such as 1ES 1218+304, the duration of a flare is a few days, but some extreme blazars exhibit non-variable flux in observations that span several years, such as 1ES 0229+200. After the $\gamma\gamma$ collision, relativistic electrons scatter the CMB photons to the GeV band. The IC cooling timescale in the observer frame is

$$\Delta t_{\rm IC} \approx (1+z)\frac{t_{\rm IC}}{2\gamma_{\rm e}^2} \approx 40{\rm s}(1+z)^{-3}(\gamma_{\rm e}/10^6)^{-1}, \tag{1}$$

where $t_{\rm IC}$ is the IC cooling timescale in the source frame $t_{\rm IC} \approx 3m_{\rm e}c/(4\gamma_{\rm e}\sigma_T U_{\rm CMB}) \approx 7.7\times 10^{13}{\rm s}(1+z)^{-4}(\gamma_{\rm e}/10^6)^{-1}$ and $U_{\rm CMB} = aT^4$ is the CMB energy density. Because of the deflection effect of the IGMF, these cascade photons would reach observers after a time delay

$$\Delta t_B \approx (1+z)\frac{\lambda_{\gamma\gamma}\theta_B^2}{2c}\left(1-\frac{\lambda_{\gamma\gamma}}{D}\right) = (1+z)\frac{1}{\eta}\frac{\lambda_{\gamma\gamma}\theta_{\rm e}^2}{2c}, \tag{2}$$

where $\lambda_{\rm IC} = ct_{\rm IC}$ is the IC cooling distance of electron-positron pairs in CMB, and $\theta_{\rm e}$ is the source emitting angle. $\eta = \max(1-1/\tau_{\gamma\gamma}, 0^+)$, when $\tau_{\gamma\gamma}(E_\gamma) \to 1$ and $\lambda_{\gamma\gamma}(E_\gamma) \to D$. Only a few cascade photons along the line of sight can be observed, and most cascade photons from other directions would never be detected, thus $\Delta t_B \to \infty$. θ_B is the deflection angle

$$\theta_B \approx \begin{cases} \lambda_{\rm IC}/r_{\rm L} & \text{if } \lambda_{\rm IC} < \lambda_{\rm coh}, \\ \sqrt{\lambda_{\rm coh}/\lambda_{\rm IC}}\,\lambda_{\rm IC}/r_{\rm L} & \text{if } \lambda_{\rm IC} > \lambda_{\rm coh}, \end{cases} \tag{3}$$

where $\lambda_{\rm coh}$ characterizes the typical distance over which the magnetic field direction makes a notable change, $r_{\rm L} = \gamma_{\rm e}m_{\rm e}c^2/eB \approx 550\,{\rm Mpc}(\gamma_{\rm e}/10^6)(B/10^{-18}{\rm G})^{-1}$ is the Larmor radius of the electrons, and B is the strength of the IGMF. In this paper, we assume the correlation length is larger than 1 Mpc, that is $\lambda_{\rm IC} < \lambda_{\rm coh}$.

For a blazar flare during $t_{\rm var}$, we can treat the cascade photons as a photon shell with thickness $ct_{\rm var}$. Because of the time delay effect, at some time t, the observed cascade photons from one flare can be detected in the extended angle range $(\theta_{\rm in}, \theta_{\rm out})$, where

$$\begin{cases} \theta_{\rm out}(t) = \sqrt{2\eta ct/\lambda_{\gamma\gamma}}\,, \\ \theta_{\rm in}(t) = \sqrt{2\eta c(t-t_{\rm var})/\lambda_{\gamma\gamma}}\,. \end{cases} \tag{4}$$

Here $0 \le \theta_{\rm in}(t) < \theta_{\rm out}(t) \le \max(\theta_j, \theta_B)$. We assume that $\theta_j = \max(\theta_{j,0}, 1/\Gamma_B) = 0.1\,{\rm rad}$ in this paper. Note that the photon flux emitted from electron-positron pairs would not be diffused when $\theta_B < \theta_j$, because all the observed cascade photons are emitted from the inner part of the deflection angle θ_B, and the electrons outside θ_B would be deflected into this observable angle.

For small z, the pair-production distance $\lambda_{\gamma\gamma} \approx D/\tau_{\gamma\gamma}$, where D is the distance from the VHE source to the Earth, and the optical depth of a γ-ray photon at an observed energy E_γ, emitted by a source at redshift z, is given by

$$\begin{aligned} \tau_{\gamma\gamma}(E_\gamma, z) = & \int_0^z dz'\frac{dl}{dz'}\int_{-1}^{1} d\mu\frac{1-\mu}{2} \\ & \times \int_{\epsilon'_{th}}^{\infty} d\epsilon\, n_\epsilon(\epsilon, z')(1+z')^3\sigma_{\gamma\gamma}(\beta', z')\,, \end{aligned} \tag{5}$$

where $n_\epsilon(\epsilon, z) \equiv dn(\epsilon, z)/d\epsilon$ is the specific comoving number density of background photons with energy ϵ at redshift z. The pair-production threshold energy is $\epsilon'_{th} = 2(m_{\rm e}c^2)^2/E_\gamma(1-\mu)(1+z)$. $\sigma_{\gamma\gamma}$

is the cross-section for the $\gamma-\gamma$ interaction. The parameter $\beta'=(1-\epsilon'_{th}/\epsilon)^{1/2}$. $dl/dz=c|dt/dz|$, where l is the proper distance. Thus we can calculate the optical depth with respect to TeV photons from cosmological distant sources via the comoving specific photon number density $n_\epsilon(\epsilon,z)$, as a function of redshift. This is related to the EBL intensity $I_\nu(\nu,z)$ given by the EBL models and observations, that is

$$\epsilon^2 n_\epsilon(\epsilon)=\frac{4\pi}{c}\nu I_\nu(\nu,z)\,. \tag{6}$$

In this paper, we adopt the EBL model reported by Franceschini et al. (2008). The recent report of Ackermann et al. (2012) analyzed 150 blazars observed by Fermi/LAT, and their detected energies are above 3 GeV, covering a redshift range of 0.03 to 1.6. After assuming that $\tau_{\gamma\gamma}(E_\gamma,z)=b\times\tau_{\gamma\gamma}^{\rm model}(E_\gamma,z)$, it gave the maximum likelihood values and 1σ confidence ranges for the opacity scaling factor, $b=1.02\pm0.23$, for the EBL model of Franceschini et al. (2008).

For ultra-relativistic electrons from a $\gamma\gamma$ collision with the distribution $dN_{\rm e}/d\gamma_{\rm e}$, the time-dependent scattered photon spectrum can be given by

$$\frac{dN_\gamma^{\rm SC}}{dE_\gamma^{\rm sc}}(t)=\int d\gamma_{\rm e}\int_0^{\max(\theta_j,\theta_B)}\left(\frac{dN_{\rm e}}{d\gamma_{\rm e}}(t-\Delta t_B)\right)\left(\frac{dN_{{\rm e},\epsilon}}{dtdE_\gamma^{\rm sc}}\right)\frac{dt}{d\theta}d\theta, \tag{7}$$

where $dt/d\theta=\gamma_{\rm e}m_{\rm e}c/eB$, corresponding to the differential deflection angle $d\theta$ of the electrons moving during differential time dt in the IGMF, and $E_\gamma^{\rm sc}$ is the externally scattered photon energy. For the variable flux of a blazar flare,

$$\begin{aligned}&\int_0^{\max(\theta_j,\theta_B)}\left(\frac{dN_{\rm e}}{d\gamma_{\rm e}}(t-\Delta t_B)\right)_{\rm tot}\left(\frac{dN_{{\rm e},\epsilon}}{dtdE_\gamma^{\rm sc}}\right)\frac{dt}{d\theta}d\theta\\&\quad=\int_{\theta_{\rm in}(t)}^{\theta_{\rm out}(t)}\left(\frac{dN_{\rm e}}{d\gamma_{\rm e}}\right)_{\rm flare}\left(\frac{dN_{{\rm e},\epsilon}}{dtdE_\gamma^{\rm sc}}\right)\frac{dt}{d\theta}d\theta\\&\qquad+\int_0^{\max(\theta_j,\theta_B)}\left(\frac{dN_{\rm e}}{d\gamma_{\rm e}}\right)_{\rm continuity}\left(\frac{dN_{{\rm e},\epsilon}}{dtdE_\gamma^{\rm sc}}\right)\frac{dt}{d\theta}d\theta\,,\end{aligned} \tag{8}$$

where the total electron spectrum consists of the flare component that could be treated as a shell and the continuous component. For the flare component, due to the time delay effect, the observed cascade flux of the flare component comes from a ring of the flare shell. After the flare "trigger," the cascade flux from high latitudes gradually grows and reaches its maximum flux at the minimum time the occurs at the end of the flare and Δt_B. After the flare ends, the cascade flux from low latitudes reduces, and finally it terminates on the edge of $\max(\theta_j,\theta_B)$. On the other hand, for the continuous component, if $\theta_j<\theta_B$, the cascade flux would be diffused by a factor, θ_j/θ_B, due to the fact that the jet angle of the blazar is diffused by IGMF to a larger angle θ_B, shown in Figure 1. Note that the diffused deflection angle is proportional to θ_B rather than θ_B^2, since the deflection caused by the IGMF is in the plane of the magnetic field and the electron velocity. However, if $\theta_j>\theta_B$, the electron flux with the same energy does not diffuse by the IGMF, due to all observed cascade photons coming from the θ_B emission angle. The single electron spectrum of the IC process is (Blumenthal & Gould 1970),

$$\frac{dN_{\gamma_{\rm e},\epsilon}}{dtdE_\gamma^{\rm sc}}=\frac{\pi r_0^2 c}{2\gamma_{\rm e}^4}\frac{n(\epsilon)d\epsilon}{\epsilon^2}\left[2E_\gamma^{\rm sc}\ln\left(\frac{E_\gamma^{\rm sc}}{4\gamma_{\rm e}^2\epsilon}\right)+E_\gamma^{\rm sc}+4\gamma_{\rm e}^2\epsilon-\frac{E_\gamma^{\rm sc2}}{2\gamma_{\rm e}^2\epsilon}\right], \tag{9}$$

which is the spectrum of photons scattered (using the Thomson cross-section formula) by an electron with a Lorentz factor of $\gamma_{\rm e}$, and the differential number density of the CMB photon gas is

$$n(\epsilon)=\frac{1}{\pi^2(\hbar c)^3}\frac{\epsilon^2}{\exp(\epsilon/kT)-1}\,. \tag{10}$$

The spectrum of the electron-positron pairs can be evaluated as follows. For a primary fluence dN_γ/dE_γ, the associated flux of secondary pairs is

$$\frac{dN_{\rm e}}{d\gamma_{\rm e}} = 4m_{\rm e}c^2\frac{dN_\gamma}{dE_\gamma}\left[1-{\rm e}^{-\tau_{\gamma\gamma}(E_\gamma,z)}\right] . \quad (11)$$

Due to the IGMF deflecting the paths of the pairs, the cascade emission appears as an extended emission around the initial point source. The observed photons from cascade emission should be produced at (Dermer et al. 2011)

$$\lambda_{\gamma\gamma} < \lambda_{\rm PSF} \approx D\,\theta_{\rm PSF}/\theta_B\,, \quad (12)$$

where $\theta_{\rm PSF}$ is the PSF of Fermi/LAT. Only the electrons satisfying the above equation contribute to the cascade flux in the PSF of LAT.

3 PRIMARY EMISSION SPECTRUM

In this work, we use the publicly available data of the Fermi/LAT, contemporaneous with TeV observations, as mentioned by Şentürk et al. (2013). We use the instrument response functions $P7SOURCE\_V6$ and analyze these data via the Fermi Science Tools $v9r27p1$ software package, adopting the class 2 events. We select photons with energies in the $0.1-300\,{\rm GeV}$ range for the analysis. During the spectral fitting, we analyze all the sources listed in the Fermi two-year catalog and fit them via the software package $SED_{scripts}\_v13.1$, using the current Galactic diffuse emission model $gal\_2yearp7v6\_v0$ and the isotropic model $iso\_p7v6source$ in a likelihood analysis. As pointed out by Şentürk et al. (2013), seven cases (RGB J0710+591, 1ES 1218+304, PKS 1222+21 (4C +21.35), PKS 1424+240, PKS 2155-304, and two different measurements of 3C 66A) were the VHE data found during the first 27 months that Fermi collected data, and the remainder of the VHE data were taken before the Fermi mission (Şentürk et al. 2013). In this paper, we consider two cases, non-variable extreme blazars, e.g. 1ES 0229+200, and flaring blazars, e.g. 1ES 1218+304.

The TeV blazar 1ES 0229+200 ($z=0.14$) was observed with H.E.S.S. in 2005 and 2006, and with VERITAS (Perkins & VERITAS Collaboration 2010) in 2009 and 2010 (Vovk et al. 2012), and the VHE flux of the source has been observed to be stable for more than three years, which presently provides the strongest constraints on the lower limits of the IGMF. The observed highest energy is $E_{\rm max}=15\,{\rm TeV}$. No evidence for variability of the TeV flux has been reported, so the observations give an average TeV flux from this source on timescales of $\approx 3\,{\rm yr}$, though with poor sampling. On the other hand, correcting the observed TeV spectrum for $\gamma\gamma$ absorption, even by the lowest plausible level of the EBL, provides evidence for a very hard (photon spectral index $\Gamma_{\rm ph}\lesssim 1.5$) intrinsic source spectrum out to TeV energies, which is contrary to the SSC radiation mechanism ($\Gamma_{\rm ph}\gtrsim 1.5$). One way to overcome this problem could be that there is an additional and very hard spectral component emerging above the SSC emission at those photon energies. Böttcher et al. (2008) proposed that a component could be produced through CMB photons Compton upscattering in the extended region of a blazar jet, and obtained the radiative cooling timescale $t_{\rm dur}\approx 750/[(\Gamma/10)^2\sqrt{E({\rm TeV})}]\,{\rm yr}$ (Dermer et al. 2011; Böttcher et al. 2008). Such a timescale may explain the non-variable TeV emission for 1ES 0229+200. For these non-variable hard TeV blazars, we assume that their TeV luminosity varies slowly during their lifetimes, in which their intrinsic photon spectral index $\Gamma\sim 1.5$. 1ES 0229+200 is not in the Fermi two-year catalog. Some papers provided upper limits in the LAT band. In this paper, we use publicly available data over the period from January 2009 to May 2013, and a region of interest with a 5° radius was selected. The light curve did not display an obvious flare, and the test statistic (TS) value found in the likelihood analysis is ${\rm TS}=31.3$.

The TeV blazar 1ES 1218+304 ($z=0.182$) was one of the extreme blazars that exhibits unusually hard VHE spectra considering the EBL absorption. Generally, TeV flares are quite common in many nearby blazars, such as Mrk 501 and Mrk 421. VERITAS data revealed a prominent flare

from 1ES 1218+304, with the flux reaching 20% of the Crab during 2009 January 30 (Acciari et al. 2010). However, the Fermi/LAT data did not show an obvious flare, contemporaneous with TeV observations (Şentürk et al. 2013). Both high state and low state spectra could be described by a power law. The observed VHE spectral index is $\Gamma \sim 3$ in the high state and the low state, and the flux of the high state is twice that in the low state. Here, we use publicly available data over the period from 2008 December 29 to 2009 April 23, which were contemporaneous with the TeV flare via the VERITAS observation. We consider a region of interest of 15°, and the TS value found in the likelihood analysis is $\mathrm{TS} = 91.4$.

In our calculations we consider the suppression of the cascade emission by the time delay effects (Plaga 1995; Dai et al. 2002) and the extended halos (Neronov & Semikoz 2009; Neronov & Vovk 2010) in our unified semi-analytical model. For 1ES 0229+200, the TeV emission was observed to be stable on a timescale of $> 3\,\mathrm{yr}$, thus the suppression of the cascade flux is led by the extended halos. For 1ES 1218+304, a TeV flare appears with a duration of a few days (Acciari et al. 2010), so that the time delay effect also makes a contribution to the suppression of the cascade flux. The details will be discussed in Section 5.

4 RESULTS

The SED of these TeV blazars found from the LAT data is shown together with the VHE spectrum at higher energies. Generally, for extragalactic TeV blazars, the source spectrum in the Fermi/LAT GeV energy band has two contributions: the primary γ-ray emission from the extreme blazar and the cascade radiation developing in intergalactic space. The different possibilities for which one of the two components in the spectrum is dominant can be illustrated for different intrinsic spectrum indexes. These extreme blazars exhibit unusually hard intrinsic power-law energy spectra, $dN/dE \propto E^{-\Gamma_i}$, after correcting for the cascade absorption by the EBL. However, as pointed out by Acciari et al. (2010), the measured spectral indices, Γ_m, of these extreme blazars range from 2.5 to 3.1, and the absorption-corrected spectral indices suggest very hard intrinsic spectra in the VHE regime with $\Gamma_i \leq 1.3$. Due to the cascade photons mainly being dominant in the GeV band, the assumption of the intrinsic index would affect the constraint on the IGMF, where the GeV flux with a harder intrinsic index needs more contributions from the cascade, leading to a weaker strength for the IGMF. Both 1ES 0229+200 and 1ES 1218+304 are considered in the soft case and the hard case. In the soft case, the intrinsic GeV spectrum dominates, and in the hard case, the cascade GeV spectrum dominates.

The SED of 1ES 0229+200 found from the LAT data is shown in Figure 2 together with the H.E.S.S. spectrum at higher energies. We assume that the intrinsic source spectrum has a high-energy cutoff at $E_{\mathrm{cut}} = 5\,\mathrm{TeV}$, for different intrinsic spectral indices, e.g. $\Gamma = 1.5$ in the soft case and $\Gamma = 1.2$ in the hard case. Note that in order to minimize the cascade emission, aimed at derivation of constraints on the IGMF, we have assumed that the intrinsic highest energy is the observed highest energy $E_{\mathrm{max}} = 15\,\mathrm{TeV}$.

In the left panel of Figure 2, for the soft case with $\Gamma = 1.5$, the main contribution to the Fermi/LAT GeV flux is given by the primary flux of 1ES 0229+200. A sufficiently strong IGMF would suppress the cascade component. If the IGMF is weaker than $10^{-13} \sim 10^{-14}\,\mathrm{G}$, then the flux of the cascade emission will be larger than that of the primary emission. In this soft case, IGMF with $\gtrsim 10^{-13}\,\mathrm{G}$ is needed to effectively suppress the cascade emission down to the level of the LAT measurements in the 0.1–300 GeV range. On the other hand, if the IGMF is weaker than $\sim 10^{-13}\,\mathrm{G}$, then the flux of the cascade emission will be the dominant contribution to the observed spectrum, instead of the primary emission of the source in the soft case, as shown in the right panel of Figure 2. If the observed GeV photons mainly come from the cascade emission, the intrinsic spectrum of the source has to have a slope harder than $\Gamma = 1.5$, the same as in Vovk et al. (2012). Here we assume $\Gamma = 1.2$. In order to make the cascade emission consistent with observations, we change the strength of IGMF to fit the observed data, and obtain some allowed ranges of IGMF strengths in the hard

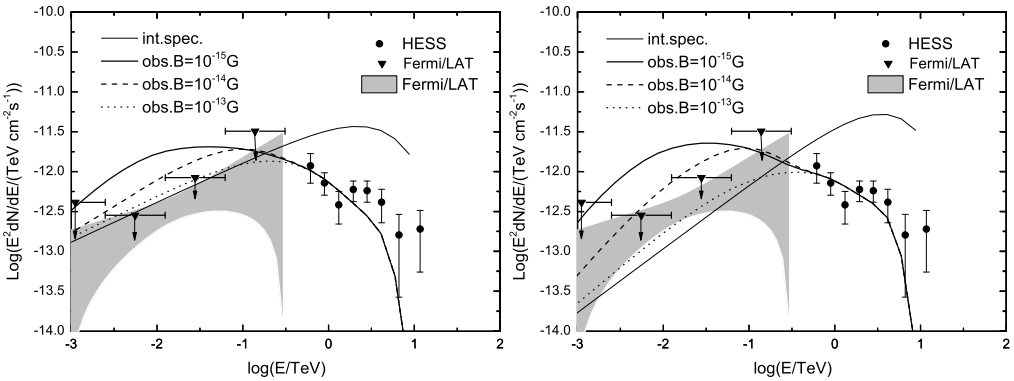

Fig. 2 The GeV-TeV SED for 1ES 0229+200 for different indexes (*left panel*: $\Gamma = 1.5$ and *right panel*: $\Gamma = 1.2$) of an intrinsic source spectrum. Lines for different values of the IGMF strength represent the sums of the intrinsic spectrum and the corresponding predicted cascade emission. We plot the Fermi/LAT data from January 2009 to May 2013. The butterfly plot was fit with $\mathrm{TS} = 31.3$. We assume that the duration time of these extreme blazars is larger than 10^6 yr with the non-variable intrinsic flux.

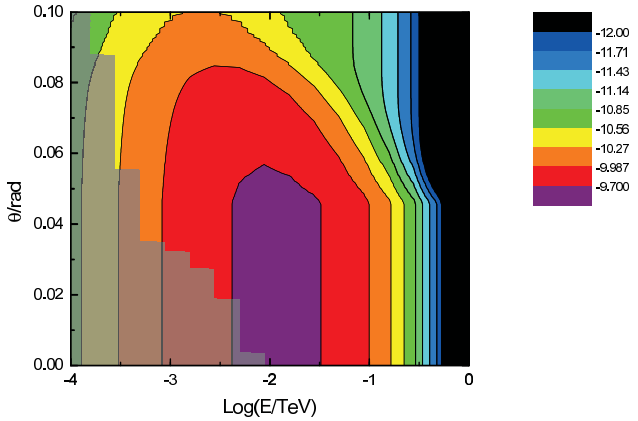

Fig. 3 The extended halo of the cascade photons for 1ES 0229+200 for different values of the cascade photon energy. We assume that the duration time of these extreme blazars is 10^7 yr. With the non-variable intrinsic flux, the IGMF strength is 10^{-14} G and the intrinsic index is $\Gamma = 1.5$. This extended halo shows that the cascade photons from lower energy electrons would come from a larger extended angle. The transparent gray area represents the PSF of Fermi/LAT, and we do not consider the upper limit of flux in this figure. The values corresponding to different colors indicate the fraction of the logarithmic intensity emitted in this deflection angle.

case. On the other hand, the lower limit of the IGMF can also be constrained by the extended halo (Neronov & Vovk 2010; Tavecchio et al. 2010; Dolag et al. 2011). Here, we also obtain the extended halo of the cascade photons as shown in Figure 3. Note that the gray area is limited by the PSF of Fermi/LAT, and the upper limit of the Fermi/LAT is only considered in the SEDs. In fact, all the data are the upper limits of the GeV band, thus the extended halo, shown in Figure 3, could not be imaged by Fermi/LAT.

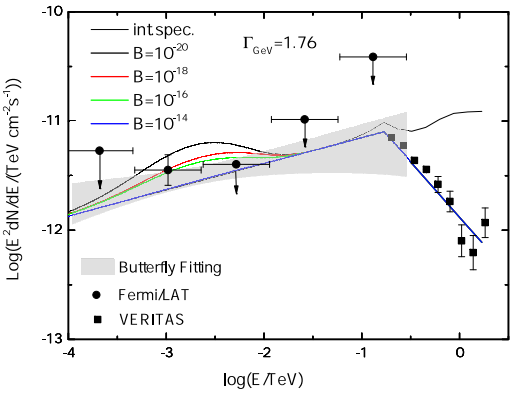

Fig. 4 The GeV-TeV SED for 1ES 1218+304 for different strengths of the IGMF with intrinsic index $\Gamma = 1.76$. Lines for different values of the IGMF strength represent the sums of the intrinsic spectrum and the corresponding predicted cascade emission. We plot the Fermi/LAT data from December 2008 to April 2009. The butterfly plot was fit with $\mathrm{TS} = 91.4$. This result represents the suppression of the IGMF. The time delay effect changes the SED from $10^{-18} \sim 10^{-20}$ G and the extended halo effect changes the SED from $10^{-14} \sim 10^{-16}$G.

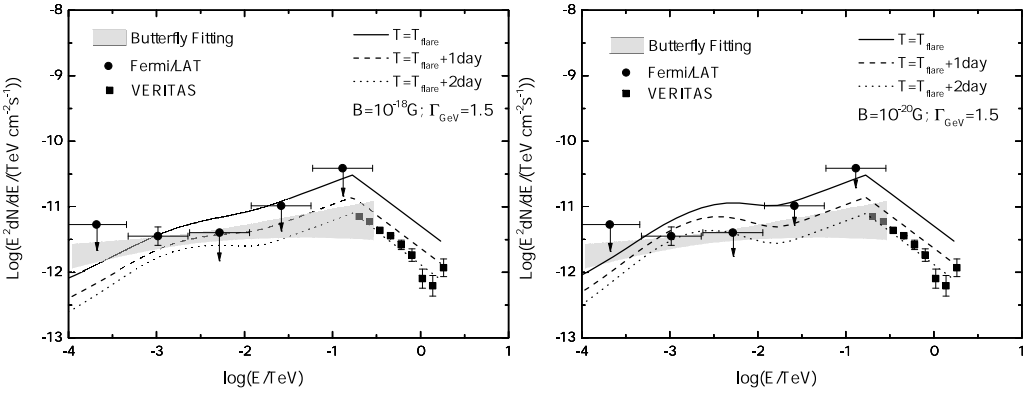

Fig. 5 The GeV-TeV SED for 1ES 1218+304 for a different strength of the IGMF with intrinsic index $\Gamma = 1.5$. Lines for different observed times represent the sums of the intrinsic spectrum and the corresponding predicted cascade emission. We plot the Fermi/LAT data from December 2008 to April 2009. The butterfly plot is fit with $\mathrm{TS} = 91.4$. *Left panel*: the strength of IGMF is 10^{-18} G. *Right panel*: the strength of IGMF is 10^{-20} G.

For 1ES 1218+304, the SED is found from the LAT data over the period contemporaneous with the VERITAS observations. We calculate the time-averaged SED from MJD 54829 to MJD 54944, shown in Figure 4. The suppression of the IGMF could consist of two components: the flux of the flare, from $10^{-18} \sim 10^{-20}$ G, and the flux of the nonflare state, from $10^{-14} \sim 10^{-16}$ G. The details are discussed in Section 5. After assuming the index of the high state is equal to that in the low state, we can calculate the SED at different times, shown in Figure 5, and the integral flux, obtaining the light curve shown in Figure 6 and Figure 7. Figure 5 shows how the SEDs evolve during the high state of this flare for different IGMF strengths after assuming that the index of the intrinsic spectrum

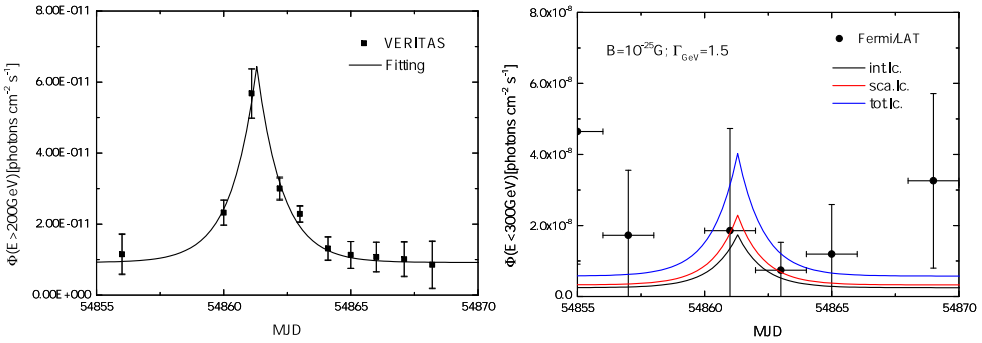

Fig. 6 *Left panel*: the light curve of VERITAS for 1ES 1218+304 from MJD54855 to MJD54870. The observed data represent the integrated flux above 200 GeV. The flux variations for the flare can be described by an exponential function $\exp(-\mid t - \mathrm{MJD}54861.3 \mid /1\,\mathrm{day})$. *Right panel*: the light curve for 1ES 1218+304 for IGMF strength $B = 10^{-25}$ G. Fermi/LAT data represent the integral flux from 0.1 GeV to 300 GeV, and the intrinsic index is $\Gamma = 1.5$. The solid line represents the intrinsic GeV light curve. The red line represents the cascade GeV light curve. The blue line represents the total GeV light curve. The strength of the IGMF is too low for the light curve of the cascade photons to show the time delay effect.

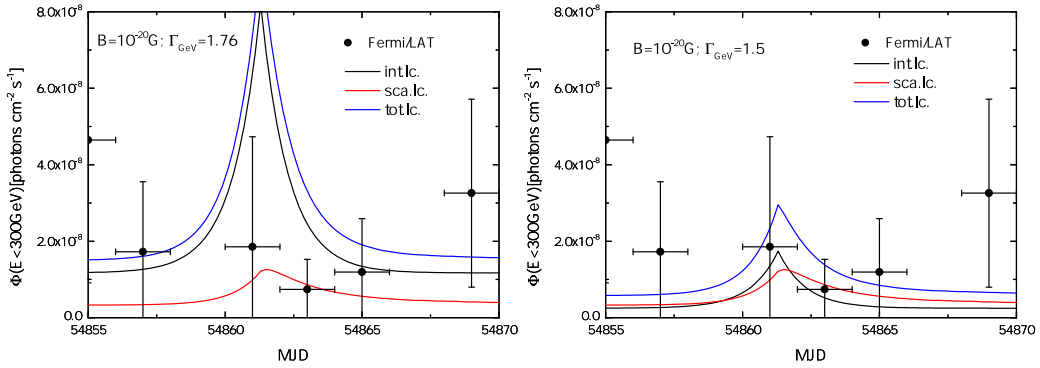

Fig. 7 *Left panel*: same as Figure 6 but for $\Gamma = 1.76$ and $B = 10^{-20}$ G. *Right panel*: same as Figure 6 but for $\Gamma = 1.5$ and $B = 10^{-20}$ G.

did not change. The GeV flux would be larger than that in the average state, but as the event rate is low over the period, we cannot exactly obtain the high state flux observed by Fermi/LAT. As shown in the left panel of Figure 7, if the strength of the IGMF is lower than 10^{-20} G and the SED is soft ($\Gamma \gtrsim 1.76$), the cascade flux could be ignored, so that the observed flux is mainly equal to the primary flux. However, if the strength of IGMF is almost zero and the SED is hard ($\Gamma \lesssim 1.5$), then the cascade flux plays the same role in the primary flux, as shown in the right panel of Figure 6. Alternately, if the strength of the IGMF is larger than 10^{-20} G and the SED is hard ($\Gamma \lesssim 1.5$), the time delay effect of the cascade flux would become obvious.

5 DISCUSSIONS AND CONCLUSIONS

Both the time delay and extended halo contribute to suppression of the cascade emission. For non-variable TeV sources, we need not consider the time delay effect because the extended halo leads to a

cascade flux lower than that in a zero magnetic field situation. Compared to Tavecchio et al. (2010); Dermer et al. (2011), we give a larger lower limit for the IGMF, on the order of $B \gtrsim 10^{-13} \sim 10^{-14}$ G after considering the diffusion of electron flux. As shown in Figure 1, here we emphasize that the cascade photons emitted from electron-positron pairs with the same energies do not diffuse by the IGMF when $\theta_j > \theta_B$, because all observed cascade photons come from the θ_B emission angle, and the other electrons outside θ_B would be deflected into it for the duration of the flare; that is, the cascade flux would not be effectively diffused. However, if $\theta_j < \theta_B$, the cascade flux would be diffused by a factor, θ_j/θ_B, due to the fact that the jet angle of the blazar is diffused by IGMF to a larger angle θ_B. Note that the diffused deflection angle is proportional to θ_B rather than θ_B^2, since the deflection caused by the IGMF is in the plane of the magnetic field and the electron velocity. Note that we assume that the primary luminosity has a uniform angular distribution, or more accurately, it should be multiplied by a factor of δ^4 for the integrated flux, where δ is the beaming Doppler factor of the blazar.

Generally, the suppression of the cascade flux caused by the IGMF has two components: The first one is the flare flux suppression. Due to the time delay, only the cascade photons in the observed time could be detected (Dai et al. 2002; Fan et al. 2004), and the recent works also report the constraint on the IGMF via a flare that lasts several days flare from a TeV blazar, such as Mrk 501 (Takahashi et al. 2012) and Mrk 421(Takahashi et al. 2013). The second one is the stable flux suppression caused by the extended halo. The non-variable extreme blazar 1ES 0229+200 gives the strongest constraints (Neronov & Vovk 2010; Tavecchio et al. 2010; Vovk et al. 2012; Dolag et al. 2011). In this paper, we described a unified interpretation for the time delay and extended halo in a semi-analytical model, and obtained a stronger constraint, on the order of $10^{-13} \sim 10^{-14}$ G, after considering the electron flux diffusion. In order to make a brief discussion, here we assume that the non-variable flux of 1ES 0229+200 is observed during a high state that lasts 100 days As shown in Figure 8 during the flare period, there are two contributions, the first one changes the cascade flux from $10^{-16} \sim 10^{-18}$ G and the second one changes it below 10^{-15} G. On the other hand, during the low state period after the flare, the suppression of the flare flux is not so obvious, so only the second one should be considered. Due to the time delay, the cascade flux from the halo at high latitudes gradually grows after the flare "trigger" and reaches its maximum flux at the minimum time of the end of the flare and Δt_B, and after the flare, the cascade flux from low latitudes reduces, and finally it terminates on the edge of the extended halo, as shown in Figure 9.

As pointed out by Vovk et al. (2012), we also emphasize that the constraint on the IGMF is in the "$B_{IGMF} - \Gamma - EBL$" parameter space, which is determined by the intrinsic properties of extreme blazars. If the intrinsic index of the GeV flux is hard, ~ 1.5, then the flux of the cascade emission will be the dominant contribution to the observed spectrum, instead of source primary emission in the soft case. In fact, we could not distinguish between the cascade photons and the intrinsic photons from the observed GeV flux, but the simultaneity of the VHE observations and the HE observation would help us to understand the composition of the GeV flux due to the time delay shown in the light curves. For most GeV flares observed by Fermi/LAT without TeV observations, one way to analyze the IGMF is calculating the time delay for different energy channels via the autocorrelation, which would be more direct evidence of the time delay. In the flare case, if the intrinsic SED is soft ($\Gamma = 1.76$ for 1ES 1218+304), the observed GeV flux is much less than the intrinsic flux so that the total flux would be variable contemporaneous with the VHE flux, without an obvious time delay effect. However, in the hard case ($\Gamma = 1.5$), the cascade flux would be larger than the intrinsic flux. In order to fit the observed GeV flux, the cascade component should be suppressed by the IGMF, on an order of $\gtrsim 10^{-18}$ G. If the strength of the IGMF is larger, the suppression of the cascade flux would be led by the extended halo effect.

For these extreme blazars, the EC model (Böttcher et al. 2008) explains well their hard TeV indexes and non-variable fluxes that last a few years. However, if we could find the TeV flux evolution from high state to low state or a flare, then the Fermi/LAT observations would give us a better chance

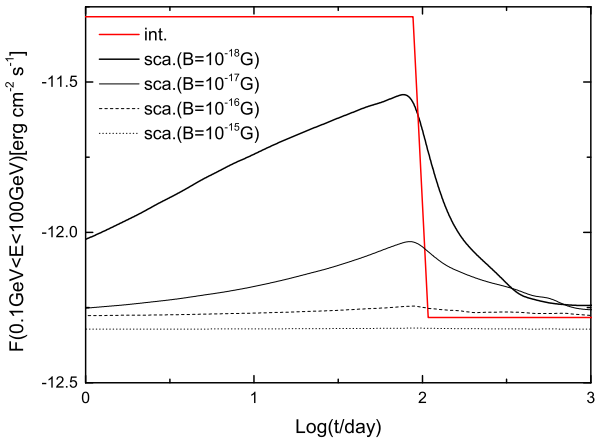

Fig. 8 The light curve of the cascade energy flux for 1ES 0229+200 for different values of the IGMF strength. We assume that the high state with non-variable flux for these extreme blazars is 100 days, and the intrinsic index is $\Gamma = 1.5$. The cascade energy flux is integrated from 0.1 GeV to 300 GeV. This result also represents the suppression of the IGMF with time delay and extended halo.

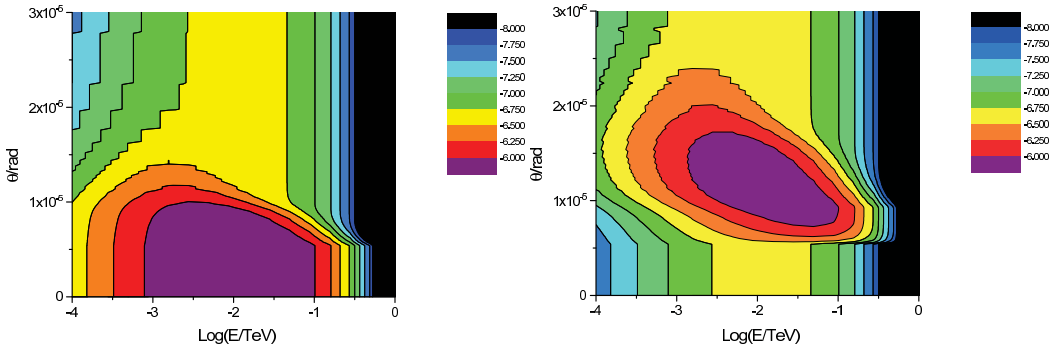

Fig. 9 The extended halo of the cascade photons for 1ES 0229+200 for different values of energy for the cascade photon. We assume that the duration time of these extreme blazars is 100 days with the non-variable intrinsic flux. The IGMF strength is 10^{-18} G and the intrinsic index is $\Gamma = 1.5$. The values corresponding to different colors indicate the fraction of the logarithmic intensity emitted in this deflection angle. *Left panel*: the observed time is assumed to be 50 days. *Right panel*: the observed time is 150 days.

to study the IGMF. On the other hand, the proton-induced intergalactic cascade emission could also be responsible for the observed hard TeV emission (Essey et al. 2010; Essey & Kusenko 2010; Essey et al. 2011), which is different from the physical process discussed in this paper.

Our results are only valid for a large correlation length ($\lambda_{\rm coh} > 1\,{\rm Mpc}$) of the IGMF. For $\lambda_{\rm coh} < 1\,{\rm Mpc}$, which scales approximately as $\lambda_{\rm coh}^{-1/2}$ as illustrated in Equation (3), because electron-positron pairs would randomly walk through the IGMF domains and the deflection angle would become smaller, a larger cascade flux and a more stringent lower limit on IGMF would appear.

Acknowledgements This work was supported by the National Basic Research Program of China (973 Program) under grant 2014CB845800 and the National Natural Science Foundation of China under grant No. 11033002. We thank Bing Zhang for discussions and help with the prose.

References

Acciari, V. A., Aliu, E., Beilicke, M., et al. 2010, ApJ, 709, L163
Ackermann, M., Ajello, M., Allafort, A., et al. 2012, Science, 338, 1190
Aharonian, F., Akhperjanian, A. G., Barres de Almeida, U., et al. 2007, A&A, 475, L9
Biermann, L. 1950, Zeitschrift Naturforschung Teil A, 5, 65
Blumenthal, G. R., & Gould, R. J. 1970, Reviews of Modern Physics, 42, 237
Bonafede, A., Feretti, L., Giovannini, G., et al. 2009, A&A, 503, 707
Böttcher, M., Dermer, C. D., & Finke, J. D. 2008, ApJ, 679, L9
Dai, Z. G., & Lu, T. 2002, ApJ, 580, 1013
Dai, Z. G., Zhang, B., Gou, L. J., Mészáros, P., & Waxman, E. 2002, ApJ, 580, L7
Dermer, C. D., Cavadini, M., Razzaque, S., et al. 2011, ApJ, 733, L21
Dolag, K., Kachelriess, M., Ostapchenko, S., & Tomàs, R. 2011, ApJ, 727, L4
Essey, W., Kalashev, O. E., Kusenko, A., & Beacom, J. F. 2010, Physical Review Letters, 104, 141102
Essey, W., & Kusenko, A. 2010, Astroparticle Physics, 33, 81
Essey, W., Kalashev, O., Kusenko, A., & Beacom, J. F. 2011, ApJ, 731, 51
Fan, Y. Z., Dai, Z. G., & Wei, D. M. 2004, A&A, 415, 483
Fossati, G., Maraschi, L., Celotti, A., Comastri, A., & Ghisellini, G. 1998, MNRAS, 299, 433
Franceschini, A., Rodighiero, G., & Vaccari, M. 2008, A&A, 487, 837
Han, J. L., Manchester, R. N., Lyne, A. G., Qiao, G. J., & van Straten, W. 2006, ApJ, 642, 868
Harrison, E. R. 1970, MNRAS, 147, 279
Ichiki, K., Inoue, S., & Takahashi, K. 2008, ApJ, 682, 127
Jansson, R., & Farrar, G. R. 2012, ApJ, 761, L11
Kronberg, P. P. 1994, Reports on Progress in Physics, 57, 325
Kulsrud, R. M., & Zweibel, E. G. 2008, Reports on Progress in Physics, 71, 046901
Murase, K., Dermer, C. D., Takami, H., & Migliori, G. 2012, ApJ, 749, 63
Murase, K., Takahashi, K., Inoue, S., Ichiki, K., & Nagataki, S. 2008, ApJ, 686, L67
Neronov, A., & Semikoz, D. V. 2009, Phys. Rev. D, 80, 123012
Neronov, A., & Vovk, I. 2010, Science, 328, 73
Perkins, J. S., & VERITAS Collaboration. 2010, in Bulletin of the American Astronomical Society, 42, AAS/High Energy Astrophysics Division #11, 708
Plaga, R. 1995, Nature, 374, 430
Razzaque, S., Mészáros, P., & Zhang, B. 2004, ApJ, 613, 1072
Şentürk, G. D., Errando, M., Böttcher, M., & Mukherjee, R. 2013, ApJ, 764, 119
Takahashi, K., Murase, K., Ichiki, K., Inoue, S., & Nagataki, S. 2008, ApJ, 687, L5
Takahashi, K., Inoue, S., Ichiki, K., & Nakamura, T. 2011, MNRAS, 410, 2741
Takahashi, K., Mori, M., Ichiki, K., & Inoue, S. 2012, ApJ, 744, L7
Takahashi, K., Mori, M., Ichiki, K., Inoue, S., & Takami, H. 2013, ApJ, 771, L42
Tavecchio, F., Ghisellini, G., Foschini, L., et al. 2010, MNRAS, 406, L70
Tavecchio, F., Ghisellini, G., Bonnoli, G., & Foschini, L. 2011, MNRAS, 414, 3566
Vovk, I., Taylor, A. M., Semikoz, D., & Neronov, A. 2012, ApJ, 747, L14
Widrow, L. M. 2002, Reviews of Modern Physics, 74, 775
Zweibel, E. G. 2006, Astronomische Nachrichten, 327, 505